

# Covariant-Conics Decomposition of Quartics for 2D Shape Recognition and Alignment

JEAN-PHILIPPE TAREL

Jean-Philippe.Tarel@inria.fr

*INRIA, Domaine de Voluceau, Rocquencourt, B.P. 105, 78153 Le Chesnay Cedex, France.*

WILLIAM A. WOLOVICH, DAVID B. COOPER

WaW@lems.brown.edu, Cooper@lems.brown.edu

*Division of Engineering, Brown University, Box D, Providence, RI, 02912-9104, USA*

*Received ??; Revised ??*

Editors: ??

**Abstract.** This paper outlines a new geometric parameterization of 2D curves where parameterization is in terms of geometric invariants and parameters that determine intrinsic coordinate systems. This new approach handles two fundamental problems: single-computation alignment, and recognition of 2D shapes under Euclidean or affine transformations. The approach is model-based: every shape is first fitted by a quartic represented by a fourth degree 2D polynomial. Based on the decomposition of this equation into three covariant conics, we are able, in both the Euclidean and the affine cases, to define a unique intrinsic coordinate system for non-singular bounded quartics that incorporates usable alignment information contained in the polynomial representation, a complete set of geometric invariants, and thus an associated canonical form for a quartic. This representation permits shape recognition based on 11 Euclidean invariants, or 8 affine invariants. This is illustrated in experiments with real data sets.

## 1. Introduction

Algebraic curves have proven to be powerful shape representations in model-based vision for handling the alignment and recognition of 2D shapes [7, 4, 15, 16, 13]. Shapes in 2D images are described by their boundaries, which are then represented by algebraic curves. An algebraic curve is the zero-set of a second or higher degree 2D polynomial, also called an implicit polynomial (IP) representation. For 3D data sets, the representation consists of algebraic surfaces. Curves of degree two are called conics, and those of degree four are called quartics.

Algebraic representations are related to geometric moments, but the advantage of algebraic curves is that the data point set is interpolated by the fitted representation, so it can handle missing data due to occlusion and to segmentation errors. Furthermore, the algebraic curves also handle open curve patches. As with geometric moments, algebraic representations have smoothing properties which provide robustness to data set noise and errors. They can also be used in a Bayesian recognition framework [11, 5].

A major benefit of algebraic representations is that they have invariants under Euclidean or affine transformations. These invariants are functions of the polynomial coefficients alone. For computer vision purposes, these invariants are used to recognize whether two given shapes are globally similar or not — they are shape descriptors.

Alignment is another fundamental problem in several disciplines, ranging from computer vision, robotics and medical imaging to photogrammetry. 2D-2D alignment is also referred to as shape registration in images. In 3D, several techniques can be used for pose estimation [8] and alignment, among which are Euclidean intrinsic coordinate systems [16] defined for algebraic curves. The advantage of using intrinsic coordinate systems of algebraic curves compared to the use of geometric moments is better robustness to moderate degrees of missing data and to varying density in point-sampling of boundaries, and the ability to deal with open curves. Moreover no initialization is needed.

Our approach utilizes the fact that a decomposition of quartics into covariant conics implies an object-based coordinate system (consisting of an

intrinsic coordinate center and an intrinsic coordinate orientation) and a *complete set of geometric invariants*. For a conic, its center of symmetry defines the intrinsic center, and the eigenvectors of the matrix associated with the second degree terms provide the intrinsic orientation.

The proposed decomposition is an improvement over [22, 23], where uniqueness is enforced in a linear way. Other decompositions of a quartic are possible: a decomposition into covariant conics [18] which only implies Euclidean invariants, and a decomposition into lines [19] which is less easy to interpret geometrically.

Our work can also be seen as a significant extension of [16, 15], where this concept of intrinsic coordinate system was generalized from the case of conics to the case of higher degree polynomials (with affine and Euclidean coordinate systems). Compared to previous studies, the originality of the approach consists in a geometric interpretation that allows us to make less incomplete use of polynomial coefficients. Indeed, we were influenced by the insightful geometric interpretation of the projective invariants of a conic pair outlined in [7] and by the more general treatment of invari-

ants in [12, 13]. The proposed approach provides a geometric signification of intrinsic coordinate systems and invariants for quartics.

In [13], an different approach based on a complex basis for IPs is proposed within a similar application context. With this approach, another complete set of Euclidean invariants is obtained, where alignment is better performed by using all the possible information in the algebraic curve. Unfortunately, this approach does not generalize to affine transformations. The aim of this paper is to demonstrate a meaningful approach to the calculation of a complete set of invariants via a geometric interpretation of these invariants, particularly under affine transformations. The invariants obtained are different from the classical algebraic invariants usually proposed [20], because they are not restricted to being rational and polynomial functions of the polynomial coefficients but rather are general functions involving roots and trigonometric functions as well. As a consequence, we call this new set of invariants *geometric invariants*. We want to emphasize the important fact that the geometric interpretation of these invariants implies a natural distance for comparing

two sets, which is fundamental to practical shape recognition. In contrast, the comparison of algebraic invariants is difficult due to very different order of magnitude of variations.

Here, we focus our attention only on quartics because conics are well known and can handle only alignment and invariants under Euclidean transformations. Cubics are not bounded curves, whereas in images we are mainly interested in bounded shapes. Thus, quartics are the lowest degree polynomials that describe our approach precisely in the affine case. Of course, when the object shape is close to a conic, a conic should be used as the edge model to provide robust and stable fitting. On the other hand, when the shape is very complex, a higher degree polynomial can be used. Extension of the proposed approach to higher degrees is possible. In the experiments described in this paper, only shapes well modeled by one quartic are considered.

After defining quartics and describing some well known asymptotic properties, we outline in section 2.1 how quartic curves can be obtained from a given raw data set by using a fitting algorithm. In section 3, we show how to decompose a non-

singular quartic as three covariant conics. In section 4, we use this decomposition to obtain a Euclidean canonical form for quartics. In particular, we illustrate how the intrinsic coordinate system defined on quartics is useful for alignment under Euclidean transformations. This coordinate system contains useful information for pose estimation. We also exhibit a complete set of invariants under Euclidean transformations with a natural distance measure on every invariant, which allows us to carry out recognition tasks in an efficient way. Finally in section 5, we extend these Euclidean results to affine transformations and present some experimental results concerning robustness to noise and missing data.

## 2. Quartics

### 2.1. Definition

A quartic is an algebraic curve of degree 4 in the plane, which is defined with Cartesian coordinates

$(x, y)$  by the implicit polynomial equation:

$$\begin{aligned} f_4(x, y) = & a_{40}x^4 + a_{31}x^3y + a_{22}x^2y^2 + a_{13}xy^3 + a_{04}y^4 \\ & + a_{30}x^3 + a_{21}x^2y + a_{12}xy^2 + a_{03}y^3 \\ & + a_{20}x^2 + a_{11}xy + a_{02}y^2 \\ & + a_{10}x + a_{01}y \\ & + a_{00} = 0 \end{aligned} \quad (1)$$

The number of polynomial coefficients  $(a_{ij})_{0 \leq i+j \leq 4}$  is 15. However, since the zero set of  $f_4(x, y)$  is unaffected by a multiplication by a non-zero scalar, a quartic has 14 independent degrees of freedom. The *homogeneous* polynomial  $H_4(x, y)$  of degree 4 in  $f_4(x, y)$  is called the leading form of  $f_4$ .

If  $a_{ij} = 0$  for  $i + j = 4$  and  $i + j = 3$ , the quartic becomes a conic, as defined by a polynomial function of degree 2:

$$f_2(x, y) = a_{20}x^2 + a_{11}xy + a_{02}y^2 + a_{10}x + a_{01}y + a_{00}, \quad (2)$$

which has 5 independent degrees of freedom.

## 2.2. Asymptotes

As in the case of conics, there are different kinds of quartics. For conics, it is well known that there are two different types of non-singular conics: hyper-

bolae and ellipses. A hyperbola has two asymptotes, and an ellipse has none.

The existence of asymptotes in the conic case depends on the existence or non-existence of real roots in the homogeneous leading terms. When  $y$  is very large, we have from (2):

$$\frac{f_2(x, y)}{y^2} \simeq a_{20}\left(\frac{x}{y}\right)^2 + a_{11}\frac{x}{y} + a_{02} \quad (3)$$

Therefore, if  $\theta$  is the angle of the asymptote, the cotangent  $t$  of  $\theta$  satisfies the equation:

$$a_{20}t^2 + a_{11}t + a_{02} = 0$$

In the same way, a quartic has an asymptote if and only if the following fourth degree equation has a real root (a root can be at infinity):

$$a_{40}t^4 + a_{31}t^3 + a_{22}t^2 + a_{13}t + a_{04} = 0 \quad (4)$$

Since this is a real equation, there are three cases:

- 4 real roots and therefore 4 asymptotes;
- 2 real roots and therefore 2 asymptotes;
- no real roots and no asymptotes, in which case the zero set of the quartic is bounded, i.e, the quartic curve is bounded.

### 2.3. Shape Modeling with Quartics

To align and compare two shapes described by their boundaries, input data sets are assumed to be sets of points along boundaries (see the dotted lines in Fig. 1). Before we can consider alignment and recognition, we must determine a quartic polynomial whose zero set approximates the data points. For this we use a fitting algorithm. Some algorithms [9, 15, 3, 17, 12] minimize the average squared distance from the data points to the zero set of the polynomial. The solution generally fits the data well. However, the fit is often too sensitive to noise or missing data, especially when the data set cannot be closely represented by a quartic.

Fortunately, the 3-level (3L) fitting algorithm introduced in [2] improves the stability of the result. In [14] the gradient one (G1) fitting algorithm is introduced, which is a differential version of the 3L algorithm. The effectiveness of the G1 and 3L fitting algorithms is that they achieve not only the fitting of the polynomial zero set on the data set, but also they constrain the tangent of the fitted algebraic curve to be close to the one of the

data curve at all data points. This is performed by enforcing the gradient of the fitted polynomial to have magnitude 1 and to be perpendicular to the data curve. Moreover to insure complete stability, a regularization technique must be applied in the case where not all IP coefficients are fully constrained by the data. A solution proposed in [14], is to use a Ridge Regression (RR) approach to bias the solution towards IPs with less unstable coefficients. RR-G1 and RR-3L fitting algorithms are numerically stable and repeatable, with respect to Euclidean transformations of the data set, and robust to noise and a moderate percentage of missing data. Fig. 1 illustrates the result of fitting on four different shapes defined by their data sets by quartics (the solid lines).

### 3. A Quartic Decomposition into Covariant Conics

The aim in this section, as first formulated in [23], is to rewrite the polynomial function in (1) as the product of two conics, plus a third conic, namely:

$$f_4(x, y) = g_2(x, y)g_2'(x, y) + g_2''(x, y)$$

The proposed decomposition is unique for non-singular bounded quartics and the three obtained conics are covariant under affine transformations.

### 3.1. The Leading Form

With the new variable  $t = \frac{x}{y}$ , the homogeneous leading form is rewritten as the fourth degree polynomial  $a_{40}t^4 + a_{31}t^3 + a_{22}t^2 + a_{13}t + a_{40}$ . This polynomial can always be factored as the product of two real second degree polynomials. Consequently:

$$\begin{aligned} f_4(x, y) = & a_{40}(x^2 + \alpha_{11}xy + \alpha_{02}y^2)(x^2 + \alpha'_{11}xy + \alpha'_{02}y^2) \\ & + a_{30}x^3 + a_{21}x^2y + a_{12}xy^2 + a_{03}y^3 \\ & + a_{20}x^2 + a_{11}xy + a_{02}y^2 \\ & + a_{10}x + a_{01}y \\ & + a_{00} \end{aligned} \quad (5)$$

We have assumed that  $a_{40} \neq 0$ . For a given quartic, the leading term decomposition can be computed without root extraction, by finding the 'bi-quadratic' form of the fourth degree polynomial in  $t$  (for example, see [1] p.118-121 for a description of this classic technique).

Notice that the leading form decomposition is unique for polynomials with 2 or 0 asymptotes. For quartics with 4 asymptotes, the real roots can be coupled three different ways.

### 3.2. Third Degree Homogeneous Terms

We now want to eliminate the third degree homogeneous terms by introducing linear terms  $\alpha_{10}x + \alpha_{01}y$  and  $\alpha'_{10}x + \alpha'_{01}y$  in each homogeneous quadratic factor in (5) as in [23]. After expansion, we rewrite the quartic polynomial:

$$\begin{aligned} f_4(x, y) = & a_{40}(x^2 + \alpha_{11}xy + \alpha_{02}y^2 + \alpha_{10}x + \alpha_{01}y) \\ & (x^2 + \alpha'_{11}xy + \alpha'_{02}y^2 + \alpha'_{10}x + \alpha'_{01}y) \\ & + (a_{30} - a_{40}(\alpha_{10} + \alpha'_{10}))x^3 \\ & + (a_{21} - a_{40}(\alpha'_{11}\alpha_{10} + \alpha_{11}\alpha'_{10} + \alpha_{01} + \alpha'_{01}))x^2y \\ & + (a_{12} - a_{40}(\alpha'_{02}\alpha_{10} + \alpha_{02}\alpha'_{10} + \alpha'_{11}\alpha_{01} + \alpha_{11}\alpha'_{01}))xy^2 \\ & + (a_{03} - a_{40}(\alpha'_{02}\alpha_{01} + \alpha_{02}\alpha'_{01}))y^3 + \dots \end{aligned}$$

We observe that the coefficients of the third order terms are linear functions of  $\alpha_{10}$ ,  $\alpha_{01}$ ,  $\alpha'_{10}$  and  $\alpha'_{01}$ . Consequently, we can choose the values of these terms to eliminate all the third order terms

by solving the following linear system:

$$a_{40} \begin{pmatrix} 1 & 0 & 1 & 0 \\ \alpha'_{11} & \alpha'_{01} & \alpha_{11} & \alpha_{01} \\ \alpha'_{02} & \alpha'_{11} & \alpha_{02} & \alpha_{11} \\ 0 & \alpha'_{02} & 0 & \alpha_{02} \end{pmatrix} \begin{pmatrix} \alpha_{10} \\ \alpha_{01} \\ \alpha'_{10} \\ \alpha'_{01} \end{pmatrix} = \begin{pmatrix} a_{30} \\ a_{21} \\ a_{12} \\ a_{03} \end{pmatrix} \quad (6)$$

After this computation, the quartic polynomial is decomposed as:

$$f_4(x, y) = a_{40}((x^2 + \alpha_{11}xy + \alpha_{02}y^2 + \alpha_{10}x + \alpha_{01}y) \\ (x^2 + \alpha'_{11}xy + \alpha'_{02}y^2 + \alpha'_{10}x + \alpha'_{01}y) + r_2(x, y)) \quad (7)$$

where the "remainder"  $r_2(x, y)$  is of a degree no greater than two:

$$r_2(x, y) = b_{20}x^2 + b_{11}xy + b_{02}y^2 + b_{10}x + b_{01}y + b_{00}$$

Notice that the centers  $(t_x, t_y)$  and  $(t'_x, t'_y)$  of each conic factor  $g_2$  and  $g'_2$ , respectively, can be determined by solving:

$$\begin{pmatrix} 1 & \frac{\alpha_{11}}{2} \\ \frac{\alpha_{11}}{2} & \alpha_{02} \end{pmatrix} \begin{pmatrix} t_x \\ t_y \end{pmatrix} = -\frac{1}{2} \begin{pmatrix} \alpha_{10} \\ \alpha_{01} \end{pmatrix} \quad (8)$$

since this computation is independent of the unknown constant term.

### 3.3. Uniqueness of the Decomposition

To express (7) as the product of two generic conics  $g_2$  and  $g'_2$ , we need to introduce constant terms  $\alpha_{00}$  and  $\alpha'_{00}$  into the two factors, respectively.

As in the previous section, we rewrite the quartic:

$$f_4(x, y) = a_{40}(x^2 + \alpha_{11}xy + \alpha_{02}y^2 + \alpha_{10}x + \alpha_{01}y + \alpha_{00})(x^2 + \alpha'_{11}xy + \alpha'_{02}y^2 + \alpha'_{10}x + \alpha'_{01}y + \alpha'_{00}) \\ + (b_{20} - \alpha_{00} - \alpha'_{00})x^2 + (b_{11} - \alpha'_{11}\alpha_{00} - \alpha_{11}\alpha'_{00})xy + (b_{02} - \alpha'_{02}\alpha_{00} - \alpha_{02}\alpha'_{00})y^2 \\ + (b_{10} - \alpha'_{10}\alpha_{00} - \alpha_{10}\alpha'_{00})x + (b_{01} - \alpha'_{01}\alpha_{00} - \alpha_{01}\alpha'_{00})y \\ + b_{00} - \alpha'_{00}\alpha_{00} \quad (9)$$

From section 2.1, we recall that a quartic has 14 degrees of freedom, and a conic 5. We want to decompose the quartic as the product of two conics,

plus a remainder term, which has  $14 - 5 \times 2 = 4$  degrees of freedom. Consequently, the remainder can not be a fully independent conic. Due to the multiplicative factor on the remainder,  $g'_2$



has only 3 degrees of freedom. It is possible, as shown in [22], to constrain this remainder conic to be singular (the product of two real or imaginary parallel lines). But this constraint involves resolving third degree equations, and thus the possible existence of three solutions.

We propose a different affine invariant constraint, which has the advantage of involving only linear computations. Indeed, we compute  $\alpha_{00}$  and  $\alpha'_{00}$  by constraining the remainder to be a conic with its center  $(c_x, c_y)$  at the mid-point of the line between points  $(t_x, t_y)$  and  $(t'_x, t'_y)$ . This constraint is linear because (8) is linear as a function of the conic coefficient when the center is given. Moreover, the coefficients of  $g''_2$  involved in this constraint are linear functions of  $\alpha_{00}$  and  $\alpha'_{00}$ . When an affine transformation is applied to a conic, its center is mapped by the same affine transformation, i.e the center of a conic is an affine covariant. Consequently,  $(c_x, c_y)$  is also a covariant of the two conics. This implies that our constraint on the third conic is invariant under affine transformations. With the uniqueness of the pre-

vious decomposition, this property ensures that  $g_2$ ,  $g'_2$ , and  $g''_2$  are covariant conics with respect to the affine transformation applied to  $f_4$ .

Finally, after computing  $\alpha_{00}$  and  $\alpha'_{00}$ , the quartic is decomposed into the product of two conics  $g_2$  and  $g'_2$  plus a third conic  $g''_2$ , whose center is aligned with the centers of  $g_2$  and  $g'_2$ :

$$\begin{aligned} f_4(x, y) = & a_{40}(x^2 + \alpha_{11}xy + \alpha_{02}y^2 + \alpha_{10}x + \alpha_{01}y + \alpha_{00}) \\ & (x^2 + \alpha'_{11}xy + \alpha'_{02}y^2 + \alpha'_{10}x + \alpha'_{01}y + \alpha'_{00}) \\ & + b_{20}(x + \alpha''_{11}xy + \alpha_{02}y^2 + \alpha_{10}x + \alpha_{01}y + \alpha''_{00}) \end{aligned} \quad (10)$$

We call (10) the decomposition of a quartic into three covariant conics, or its *covariant-conics decomposition*. Notice that for quartics with 2 or 0 asymptotes, the decomposition is unique. For quartics with 4 asymptotes, 3 such decompositions exist. If the uniqueness of the decomposition is true for most of the quartics with 2 or 0 asymptotes, there are special quartics in this class that do not have a unique decomposition. For instance, the decomposition is not unique when the matrix of linear system (6) cannot be inverted, or when one of the conics factors  $g_2$  and  $g'_2$  is singular (the matrix of linear system (8) cannot be inverted). Similarly to the conic case, these quartics are named singular.

### 3.4. Examples

Consider the quartic curve depicted in Fig. 2(a), which is defined by the polynomial equation:

$$\begin{aligned} f_4(x, y) = & 0.156250x^4 - 0.18750x^3y \\ & + 0.781250x^2y^2 - 0.750xy^3 + 0.6250y^4 \\ & - 1.250x^2y + 1.50xy^2 - 1.240y^3 \\ & - 0.93750x^2 + 2.250xy + 1.8750y^2 \\ & - 3.50y + 0.750 \end{aligned}$$

The ellipse factors without the constant terms are:  $g_2(x, y) = x^2 + 4.0y^2 - 8.0y$  and  $g'_2(x, y) = x^2 - 1.20xy + 1.0y^2$ . The center of  $g_2$  the largest ellipse, is at (0.0, 1.0). The center of  $g'_2$  is at (0.0, 0.0). Thus the center of  $g''_2$  is constrained to be at (0.0, 0.50). In this particular case, the constraint on  $\alpha_{00}$  and  $\alpha'_{00}$  is:

$$\begin{pmatrix} 0.30 & 0.0 \\ -0.50 & 2.0 \end{pmatrix} \begin{pmatrix} \alpha_{00} \\ \alpha'_{00} \end{pmatrix} = \begin{pmatrix} -3.60 \\ 5.20 \end{pmatrix} \quad (11)$$

By solving (11), we obtain the equations of the three ellipses shown in Fig. 2(b) :

$$g_2(x, y) = x^2 + 4.0y^2 - 8.0y - 12.0$$

$$g'_2(x, y) = x^2 - 1.20xy + 1.0y^2 - 0.40$$

$$g''_2(x, y) = 6.40x^2 + 25.60y^2 - 25.60y$$

Fig. 3 illustrates the unique covariant-conics decomposition of the quartic fit on the hiking boot of Fig. 1(c), where one conic factor is an ellipse and the other a hyperbola.

## 4. Quartics under Euclidean Transformations

Since the conic decomposition is covariant, we have transformed the problems of alignment and recognition of quartics to the equivalent problems on a set of three conics. Next we will show how to deduce a Euclidean intrinsic coordinate system for a quartic curve, and then determine a complete set of Euclidean invariants. The idea to first compute an intrinsic coordinate system, and then apply it on the curve to obtain invariants, is similar to what is used in [21] in a different (local) context for Euclidean, affine and homographic transformations.

### 4.1. Euclidean Intrinsic coordinate System of Quartics

We can rewrite every non-singular conic in the quartic decomposition (10) in its own Euclidean

intrinsic coordinate system, namely

$$\frac{X_{intr.}^2}{c_1} + \frac{Y_{intr.}^2}{c_2} - 1 = 0,$$

under the transformation

$$\begin{pmatrix} x \\ y \end{pmatrix} = \begin{pmatrix} \cos \psi & -\sin \psi \\ \sin \psi & \cos \psi \end{pmatrix} \begin{pmatrix} X_{intr.} \\ Y_{intr.} \end{pmatrix} + \begin{pmatrix} t_x \\ t_y \end{pmatrix},$$

where  $\psi$  and  $(t_x, t_y)$  are the angle and the center, respectively, of the intrinsic coordinate system of the conic expressed in the original coordinate system. Note that the square lengths  $c_1$  and  $c_2$  are intrinsic parameters of the conic under Euclidean transformations.

By using these canonical forms, we can rewrite (10) as:

$$\left(\frac{X^2}{c_1} + \frac{Y^2}{c_2} - 1\right) \left(\frac{X'^2}{c'_1} + \frac{Y'^2}{c'_2} - 1\right) + c \left(\frac{X''^2}{c''_1} + \frac{Y''^2}{c''_2} - 1\right) = 0 \quad (12)$$

where each conic is transformed as follows:

$$\begin{aligned} \begin{pmatrix} x \\ y \end{pmatrix} &= \begin{pmatrix} \cos \psi & -\sin \psi \\ \sin \psi & \cos \psi \end{pmatrix} \begin{pmatrix} X \\ Y \end{pmatrix} + \begin{pmatrix} t_x \\ t_y \end{pmatrix} \\ \begin{pmatrix} x \\ y \end{pmatrix} &= \begin{pmatrix} \cos \psi' & -\sin \psi' \\ \sin \psi' & \cos \psi' \end{pmatrix} \begin{pmatrix} X' \\ Y' \end{pmatrix} + \begin{pmatrix} t'_x \\ t'_y \end{pmatrix} \\ \begin{pmatrix} x \\ y \end{pmatrix} &= \begin{pmatrix} \cos \psi'' & -\sin \psi'' \\ \sin \psi'' & \cos \psi'' \end{pmatrix} \begin{pmatrix} X'' \\ Y'' \end{pmatrix} + \begin{pmatrix} \frac{t_x + t'_x}{2} \\ \frac{t_y + t'_y}{2} \end{pmatrix} \end{aligned} \quad (13)$$

Note that a factor  $c$  appears in (12). This factor is the weight between the pair  $(g_2, g'_2)$  and  $g''_2$ . In

the above, we assume that  $g_2$  has the largest major axis length (if ambiguous, we chose  $g_2$  to have the largest ratio of the major and minor axis lengths).

If a Euclidean transformation  $D$  is applied to the quartic,  $\psi, \psi', \psi'', (t_x, t_y)$  and  $(t'_x, t'_y)$  are mapped by  $D$ , and each Euclidean intrinsic coordinate systems is simply transformed by  $D = (R, T)$ , with  $R$  the rotation and  $T$  the translation.

A quartic has not only one but several intrinsic coordinate systems, as noted by Taubin [16]. Three are defined by the intrinsic coordinate system of each covariant conic. Another can be defined by the line through the three centers. Moreover, all linear combinations of these coordinate systems define other Euclidean intrinsic coordinate systems. Fig. 4 illustrates that the covariant-conics decomposition allows us to interpret a quartic as geometrically equivalent to 3 aligned conics.

Sometimes one or more of the covariant conics are imaginary. This means only that then we are not able to draw these conics in the plane, nevertheless all the properties we are using still exist. Therefore, this is not a limitation of the approach, since in fact, we are working on the associated quadratic form of every conic.

Notice, that we have to select one orientation of the intrinsic coordinate systems. When the two conic factors are ordered (one is larger than the other with respect to its major axis, or ratio of its major and minor axes), we will orient each major axis through the largest conic factor  $g_2$ .

Since we have several intrinsic coordinate systems, to do the alignment between two given quartics, we have to figure out what is the one to one correspondence between these intrinsic coordinate systems. To avoid the matching problem of coordinate systems, a coordinate system can be chosen in the following ways:

- if the two conic factors are non-circular, we choose the orientation of the intrinsic coordinate systems defined in Fig. 4(a). The origin of the intrinsic coordinate system is defined as the center  $(c_x, c_y)$  of the line between points  $(t_x, t_y)$  and  $(t'_x, t'_y)$ . To define the intrinsic orientation, the major axis of  $g_2$  and  $g'_2$  is first oriented as the vector defined by  $(t_x, t_y)$  and  $(t'_x, t'_y)$ . Thus, the first axis  $X_{intr}$  of the coordinate system is defined as the normalized sum of the normalized directions of the two major axes of  $g_2$  and  $g'_2$  oriented as above.

- if one of the conic factors is a circle, and the centers of the conic factors are different, the first axis  $X_{intr}$  of the coordinate system is defined as the normalized vector given by points  $(t_x, t_y)$  and  $(t'_x, t'_y)$ , and thus  $X_{intr}$  is always oriented through the conic  $g_2$ . The orientation of the intrinsic coordinate system is shown in Fig. 4(b).

In most of the other cases, one can define a unique coordinate system. The quartic reduced to a circle is a singular quartic for the computation of the coordinate system. Indeed, in such a case, there is no way to robustly extract the rotation angle.

#### 4.2. Euclidean Alignment Experiments

In this section, we present a summary of the stability experiments of the computation of the intrinsic coordinate system. Robustness to random bumps and missing data along the curves are tested separately (see Fig. 5).

For example, with the car or the hiking boot shapes of Fig. 1, using of the definition of the coordinate system of Fig. 4(a), we obtain better results than those obtained using Taubin's coordinate system or the classical scatter matrix

method, as shown in Fig. 6. Our approach performs better than the scatter matrix method because the shapes used here are not elongated, but what we will term "blobby". For elongated shapes, the alignment technique based on the fitting of a conic and the use of the Euclidean intrinsic coordinate system of this conic provides more robust and accurate results. Consequently in the Euclidean case, our approach based on quartics handles the case of blobby shapes, where conic based algorithms usually fail. Fig. 6(b) also shows that, compared to moment approaches, the fitting algorithm nicely interpolates missing data when no high curvature points are removed.

A way to check the computation of the Euclidean transformation between the original and transformed shapes is to apply the transformation on the original data point sets and then to compute the value of  $\sum_i f_4^2(R(x_i, y_i))$ . This gives us a simple estimate of a non-Euclidean distance between the polynomial function  $f_4$  and the transformed data set  $R(x_i, y_i)$ . A good estimation is associated with the smallest value [6].

We test the robustness of the estimation of the intrinsic coordinate system under noise and miss-

ing data on the 4 shapes of Fig. 1. First, we add bumps at 50 locations along the curve. The amplitude of the bump is a random Gaussian variable with a variance of 0.05. An example of a perturbed data set is shown in Fig. 5. Table 1 illustrates the robustness of the estimation of the intrinsic coordinate system under noise.

Next, we removed 5% of the length of the data at 50 different starting points. Table 1 shows that the estimation is very stable for the intrinsic angle of the boot and of the skyhawk, but less stable for the guitar and the car under 5% missing data. As shown in Fig. 5, this can be explained by the fact that removing 5% of the guitar can suppress shape features that are important to compute the pose.

#### 4.3. Euclidean Invariants of Quartics

Since there are 3 degrees of freedom in a 2D Euclidean transformation, and 14 degrees of freedom for a quartic, we want to find 11 independent invariants. The values of  $c_1, c_2, c'_1, c'_2, c''_1$  and  $c''_2$  are invariants of the conics  $g_2, g'_2$  and  $g''_2$ , hence they are Euclidean invariants of the quartic. The proof is straightforward using (12). In a similar way,  $c$

also is a Euclidean invariant, so we directly have 7 independent invariants for a quartic.

From the geometric interpretation of the quartic in terms of 3 conics, we are able to exhibit a complete set of 11 invariants for quartics. As shown in Fig. 4, there are several ways to define an intrinsic coordinate system for a quartic and, therefore, different choices for geometric invariant sets. With the definition used in Fig. 4(b), a possible set of 11 geometric invariants is as shown in Fig. 7:

- $c_1, c_2, c'_1, c'_2, c''_1$  and  $c''_2$ : squared real or imaginary lengths of minor and major axes of the three covariant conics,
- $\phi, \phi'$  and  $\phi''$ : the three angles of the major axes of the conics,
- $c_{12}$  the half length of the distance between the conic factor centers,
- and the relative weight  $c$  between the conics  $(g_2, g'_2)$  and the conic  $g''_2$  (see (12)).

The values of these 11 invariants completely specifies a quartic under Euclidean transformations.

Since the definition of these invariants involves trigonometric functions and rational roots, these 11 invariants are not classical algebraic invariants, but rather they are *geometric invariants* directly obtained from our covariant-conics decomposition. Indeed, an algebraic invariant is a function of the polynomial coefficients where only addition, subtraction, multiplication and division are involved.

We want to emphasize that these new geometric invariants (lengths and angles) are very important for recognition tasks, because they imply a natural and meaningful physical measure which can be used to discriminate between object shapes.

With (13), we can now obtain a unique canonical form for a quartic :

$$\left(\frac{X^2}{c_1} + \frac{Y^2}{c_2} - 1\right)\left(\frac{X'^2}{c'_1} + \frac{Y'^2}{c'_2} - 1\right) + c\left(\frac{X''^2}{c''_1} + \frac{Y''^2}{c''_2} - 1\right) = 0 \quad (14)$$

where we have introduced three coordinate systems  $(X, Y)$ ,  $(X', Y')$ , and  $(X'', Y'')$ . These are, respectively, the three intrinsic coordinate systems of the three covariant conics  $g_2, g'_2$ , and  $g''_2$ , defined by (see Fig. 8):

$$\begin{pmatrix} X_{intr.} \\ Y_{intr.} \end{pmatrix} = \begin{pmatrix} \cos \phi & -\sin \phi \\ \sin \phi & \cos \phi \end{pmatrix} \begin{pmatrix} X \\ Y \end{pmatrix} + \begin{pmatrix} c_{12} \\ 0 \end{pmatrix}$$

$$\begin{pmatrix} X_{intr.} \\ Y_{intr.} \end{pmatrix} = \begin{pmatrix} \cos \phi' & -\sin \phi' \\ \sin \phi' & \cos \phi' \end{pmatrix} \begin{pmatrix} X' \\ Y' \end{pmatrix} + \begin{pmatrix} -c_{12} \\ 0 \end{pmatrix}$$

$$\begin{pmatrix} X_{intr.} \\ Y_{intr.} \end{pmatrix} = \begin{pmatrix} \cos \phi'' & -\sin \phi'' \\ \sin \phi'' & \cos \phi'' \end{pmatrix} \begin{pmatrix} X'' \\ Y'' \end{pmatrix}$$

Thus, the canonical form is defined in the intrinsic coordinate system  $(X_{intr.}, Y_{intr.})$ , which is related to the original coordinate system by:

$$\begin{pmatrix} x \\ y \end{pmatrix} = \begin{pmatrix} \cos \theta & -\sin \theta \\ \sin \theta & \cos \theta \end{pmatrix} \begin{pmatrix} X_{intr.} \\ Y_{intr.} \end{pmatrix} + \begin{pmatrix} c_x \\ c_y \end{pmatrix}$$

As explained in sections 3.3 and 4.1, the covariant-conics decomposition and its coordinate system is unique for non-singular quartics with 0 or two asymptotes. Thus, the canonical decomposition is also unique for these quartics. In the case of 4 asymptotes, we can obtain a unique canonical decomposition by using the invariants. For example, one may choose the decomposition where the factor  $c$  is maximum.

Notice that, from (14), it is easy to express polynomial coefficients as functions of the geometric invariants, and then write the usual algebraic invariants as functions of the geometric invariants.

#### 4.4. Examples

Consider the decomposed quartic of section 3.4. The center  $(c_x, c_y)$  of the quartic, (the center of the two conic factor centers  $(0.0, 0.0)$  and  $(0.0, 1.0)$ ) is  $(0.0, 0.50)$ . In light of Fig. 4(b), and (14), the angle of the first axis  $X_{intr}$  of the coordinate system is  $\frac{\pi}{2}(\pi)$ . Since  $g_2$  has the larger major axis length of the two conic factors, the intrinsic coordinate system is oriented through its center. Therefore  $\theta = \frac{\pi}{2}$ . The intrinsic coordinate system of the quartic is consequently given by:

$$X_{intr.} = \cos\left(\frac{\pi}{2}\right)(x - 0.0) + \sin\left(\frac{\pi}{2}\right)(y - 0.50)$$

$$Y_{intr.} = -\sin\left(\frac{\pi}{2}\right)(x - 0.0) + \cos\left(\frac{\pi}{2}\right)(y - 0.50)$$

with the intrinsic coordinate system so defined:

$$g_2(x, y) = \frac{1}{16.0}(\cos(-\frac{\pi}{2})(X_{intr.} + 0.50) + \sin(-\frac{\pi}{2})(Y_{intr.} + 0.0))^2$$

$$+ \frac{1}{4.0}(-\sin(-\frac{\pi}{2})(X_{intr.} + 0.50)$$

$$+ \cos(-\frac{\pi}{2})(Y_{intr.} + 0.0))^2 - 1$$

$$g'_2(x, y) = (\frac{1}{1.0}(\cos(-\frac{\pi}{4})(X_{intr.} - 0.50)$$

$$+ \sin(-\frac{\pi}{4})(Y_{intr.} - 0.0))^2$$

$$+ \frac{1}{0.250}(-\sin(-\frac{\pi}{4})(X_{intr.} - 0.50)$$

$$+ \cos(-\frac{\pi}{4})(Y_{intr.} - 0.0))^2 - 1)$$

$$\begin{aligned}
g_2''(x, y) &= \frac{1}{1.0}(\cos(-\frac{\pi}{2})X_{intr.} \\
&\quad + \sin(-\frac{\pi}{2})Y_{intr.})^2 \\
&\quad + \frac{1}{0.250}(-\sin(-\frac{\pi}{2})X_{intr.} \\
&\quad + \cos(-\frac{\pi}{2})Y_{intr.})^2 - 1
\end{aligned}$$

From these equations, we deduce that  $c_1 = 16.0$ ,  $c_2 = 1.0$ ,  $c'_1 = 1.0$ ,  $c'_2 = \frac{1}{4.0}$ ,  $c''_1 = 1.0$ ,  $c''_2 = \frac{1}{4.0}$  and  $c = 1.0$ . The distance between the quartic center and one of the conic centers is  $c_{12} = 0.50$ . In the intrinsic Euclidean coordinate system, all the characteristics of the quartic are Euclidean invariants.

#### 4.5. Recognition Tests

Table 2 shows the average percentage of errors between invariants of four curves where 50 random bumps are added along the curve. The size of each bump is a random variable of standard deviation 0.05. As in the previous experiments, the average is on 20 realizations. In the right part of Table 2, the shape has missing data at different starting points. The size of the missing data length is always 5% of the curve, and the average is based on 50 different starting points. Table 2 illustrates that the computation of the geometric invariants is stable under a modest amount of noise or miss-

ing data. Note that the invariants  $c$ ,  $\phi''$ ,  $\frac{c''}{c_1}$  and  $\frac{c'_1}{c_1}$  of the skyhawk shape vary considerably. This can be explained by the fact that for this particular shape, the estimation of these invariants is very correlated because one of the two conic factors is close to a parabola. Indeed, under noise or missing data, the estimated shape can be a hyperbola as a huge ellipse, introducing instability in the invariants computation. In particular, the center is very instable in this configuration. We expect these difficulties can be solved by applying a regularization technique such as Ridge Regression.

In these experiments, we generally notice that the invariants have different robustness under missing data or noise.

In Fig. 9, the mean of the invariant  $\sqrt{|c_1|}$  and its standard deviation is shown for an increasing amount of noise. For this hiking boot shape and for this parameter, the estimation is good until the noise is more than 0.13. For bigger noise, the estimation becomes unstable. We observed the well known threshold effect [10] in estimation problems. This observation leads us to develop a more robust approach for comparing two alge-



braic curves under Euclidean transformations [13]. It relies on the translation alignment using all the information about algebraic curves, followed by the computation of a complete set of rotation invariants. If this last approach should be preferred in the Euclidean case, it does not seem to extend to the affine case, unlike the approach described here.

Fig. 10 shows how the two invariants  $(\sqrt{|\frac{c_1}{c_2}|}, \sqrt{|\frac{c'_1}{c'_2}|})$  are well separated for the four shapes of Fig. 1, so the proposed geometric invariant metric allows us to solve the recognition task.

## 5. Quartics under Affine Transformations

In this section, we apply the approach explained in the Euclidean case to the affine case. We will next show how to deduce an affine intrinsic coordinate system for a quartic curve, and then determine a complete set of affine invariants by computing the Euclidean invariants of the conics in the decomposition after transformation to the intrinsic coordinate system.

### 5.1. Affine Intrinsic coordinate System of Quartics

There is no unique affine canonical form for a conic. An infinite number of affine transformations can change a given ellipse to a circle, for example. Nevertheless, and it is one of the main reasons for using quartics, it is possible to have an affine canonical form for a quartic by using the two covariant conics to define an affine intrinsic coordinate system.

A good candidate, for the origin of this coordinate system is  $(c_x, c_y)$  the center of  $g''_2$  as described in the previous section. When the origin is known, we have to define an intrinsic coordinate system under linear transforms. First, we define  $E = \begin{pmatrix} e_{20} & \frac{e_{11}}{2} \\ \frac{e_{11}}{2} & e_{02} \end{pmatrix}$  and  $E' = \begin{pmatrix} e'_{20} & \frac{e'_{11}}{2} \\ \frac{e'_{11}}{2} & e'_{02} \end{pmatrix}$ , the matrices associated with the leading terms of each conic  $g_2$  and  $g'_2$ . These matrices are unique up to a scale factor. To define these matrices in a unique way, we assume that each conic is centered, and that its constant term is  $-1$ , before computing  $E$  and  $E'$ .

If a linear transform  $L$  is applied to the quartic, the previous two matrices become  $L^t E L$  and  $L^t E' L$ , respectively, and the product  $E'^{-1} E$  be-

comes  $L^{-1}E'^{-1}EL$ . We therefore deduce that the eigenvalues  $\lambda_i$  of  $E'^{-1}E$  are affine invariants and, moreover, that the eigenvectors  $u_i$  of this matrix are linearly transformed by an affine transformation of the coordinate system. This eigenvector problem is equivalent to the following generalized eigenvector problem:

$$Eu_i = \lambda_i E' u_i \quad (15)$$

The two eigenvectors  $u_1$  and  $u_2$ , which are solutions of (15), provide the directions of an affine intrinsic coordinate system for the quartic. However, this eigenvector problem does not always have a real solution. If the matrix  $E$  or  $E'$  is positive definite, i.e, if one of the conic factors is an ellipse, a real solution always exists. Indeed, when  $E'$  is positive definite, the square root  $B$  defined by  $E' = BB^t$  exists. Consequently, the problem is equivalent to finding the eigenvectors  $B^t u_i$  of the symmetric matrix  $B^{-1}EB^{-t}$ . Notice that in this case, the length of the vectors in the intrinsic coordinate system are also computed to transform  $g'_2$  into a unit circle.

When  $g_2$  and  $g'_2$  are two hyperbolas, the previous properties do not apply. In this case, the lead-

ing term has 4 real roots, and the decomposition is not unique. However when roots are ordered, it is not difficult to show that real eigenvectors always exist if the two conic factors involve consecutive roots.

By diagonalizing the matrix  $E'^{-1}E$ , we have the direction of each axis of the intrinsic coordinate system. If we reverse the roles of  $E$  and  $E'$ , the computed eigenvectors stay the same but the computed eigenvalues are inverted. Then, we order the axes by first choosing the axis which maximizes  $\lambda_i + \frac{1}{\lambda_i}$ , where  $\lambda_i$  is the associated eigenvalue. Moreover, if  $\lambda_1$  is less than 1, we decide that the two ellipses are in reverse order. By convention,  $g_2$  is defined as the largest conic factor. Then, both lengths of the vectors of the affine intrinsic coordinate system are computed to transform  $g'_2$  into a circle.

Therefore, we have defined the direction and the length of every axis of the affine intrinsic coordinate system. We now orient each axis through the center of the largest conic  $g_2$  (see Fig. 11). After all these steps, the coordinate system is uniquely defined for non-singular quartics with zero or two asymptotes.

### 5.2. Affine Invariants of Quartics

When an intrinsic coordinate system has been found, we apply the inverse of the affine transformation to map the origin of the coordinate system to  $(0, 0)$  and the coordinate orientations to orthogonal unit vectors. The quartic is thus set in its intrinsic coordinate system. After this transformation, the Euclidean invariants of the set of 3 conics (computed as described in section 4) are affine invariants of the original quartic.

In this case, however, not all of the Euclidean invariants are useful. We want a largest independent subset. As shown in Fig. 11, a possible set of geometric affine invariants is:

- $c_1, c_2$ : squared lengths of minor and major axes of the conic  $g_2$  (positive for ellipses and negative for hyperbolas) in the intrinsic coordinate system,
- $(t_x, t_y)$  the position of the center of the conic  $g_2$ ,
- $c_1''$  and  $c_2''$  the squared lengths of minor and major axes of the central conic  $g_2''$ ,
- $\phi''$  the angle of the major axis of  $g_2''$ ,

- and the relative weight  $c$  between the conic factors and the central one.

The number of geometric invariants is then 8.

An affine transformation has 6 degrees of freedom.

The geometric invariant set is then complete, since  $8+6 = 14$ , which is equal to the number of quartic degrees of freedom. As in the Euclidean case, the invariants obtained are different from the classical algebraic invariants.

The unique canonical form in the affine case is:

$$f_4(x, y) = \left( \frac{(X_{intr.} - t_x)^2}{c_1} + \frac{(Y_{intr.} - t_y)^2}{c_2} - 1 \right) \\ ((X_{intr.} + t_x)^2 + (Y_{intr.} + t_y)^2 - \epsilon) \quad (16) \\ + c \left( \frac{X''^2}{c_1''} + \frac{Y''^2}{c_2''} - 1 \right) = 0$$

with  $\epsilon = \pm 1$  and

$$\begin{pmatrix} X_{intr.} \\ Y_{intr.} \end{pmatrix} = \begin{pmatrix} \cos \phi'' & -\sin \phi'' \\ \sin \phi'' & \cos \phi'' \end{pmatrix} \begin{pmatrix} X'' \\ Y'' \end{pmatrix}$$

and where the intrinsic coordinate system is defined by:

$$\begin{pmatrix} x \\ y \end{pmatrix} = \begin{pmatrix} u_{1x} & u_{2x} \\ u_{1y} & u_{2y} \end{pmatrix} \begin{pmatrix} X_{intr.} \\ Y_{intr.} \end{pmatrix} + \begin{pmatrix} c_x \\ c_y \end{pmatrix}$$

The vectors  $u_1 = (u_{1x}, u_{1y})$  and  $u_2 = (u_{2x}, u_{2y})$  are the two eigenvectors of (15). Note that we have to introduce  $\epsilon$  which equals  $-1$  if  $g_2'$  is a real circle or  $+1$  if  $g_2'$  is an imaginary circle. This  $\epsilon$  is a characteristic of the quartic, but since its value

is discrete, this parameter is not included in the set of geometric invariants.

From this affine canonical form, we can express classical algebraic invariants as functions of the geometric invariants. For example, the invariant of the leading term

$$12a_{40}a_{04} - 3a_{31}a_{13} + a_{22}^2 = \frac{12}{c_1c_2} + \left(\frac{1}{c_1} + \frac{1}{c_2}\right)^2$$

which is not easy to interpret geometrically.

### 5.3. Examples

Let us consider the same quartic as in section 3.4.

In this example, we have  $E = \begin{pmatrix} 0.06250 & 0.0 \\ 0.0 & 0.250 \end{pmatrix}$

and  $E' = \begin{pmatrix} 2.50 & -1.50 \\ -1.50 & 2.50 \end{pmatrix}$  when each ellipse is centered and the constant term equals  $-1$ .

The two normalized eigenvectors are  $(E_1, E_2) = \begin{pmatrix} -0.98496 & 0.57432 \\ 0.17275 & 0.81863 \end{pmatrix}$  and the two eigenvalues are  $c_1 = 44.209$  and  $c_2 = 5.7906$ . We note that the order of the two vectors is correct, since  $c_1 + \frac{1}{c_1}$  is larger than  $c_2 + \frac{1}{c_2}$ .

Since  $(E_1, E_2)^t E' (E_1, E_2) = \begin{pmatrix} 3.01047 & 0 \\ 0.0 & 1.08953 \end{pmatrix}$ , we must divide the first and the second eigenvectors of  $(E_1, E_2)$  by the square root of the corre-

sponding diagonal element in order to transform  $g'_2$  into a circle. The resulting affine intrinsic coordinate system is:

$$\begin{pmatrix} x \\ y \end{pmatrix} = \begin{pmatrix} 0.56768 & 0.55021 \\ -0.09956 & 0.78427 \end{pmatrix} \begin{pmatrix} X_{intr.} \\ Y_{intr.} \end{pmatrix} + \begin{pmatrix} 0.0 \\ 0.5 \end{pmatrix}$$

Notice that the affine center is the same as the Euclidean center in this expression. We can check that the orientation of each vector is correct, because the two coordinates  $(t_x, t_y) = (0.55021, 0.56768)$  of the center of  $g_2$  are both positive in the intrinsic coordinate system. The quartic is shown in this intrinsic coordinate system in Fig. 12, where  $g'_2$  is transformed into a circle.

The value of the invariants shown in Fig. 11 are then computed. The square axis lengths of  $g_2$  are  $c_1 = 44.209$  and  $c_2 = 5.7906$ . The square axis lengths of  $g'_2$  are  $c'_1 = 2.7631$  and  $c'_2 = 0.36191$ . The invariant angle is  $\phi'' = 0(\pi)$ , the position of the center  $(t_x, t_y)$  is  $(0.55022, 0.56768)$ , and  $c = 1.0$ .

Finally, Fig. 13 depicts the affine canonical decomposition of the hiking boot shape, which was shown in section 4.4 for the Euclidean case.

#### 5.4. Affine Alignment

We have computed the variances of alignment and invariance errors under affine transformations with additive bumps and missing data, respectively. Fig. 14 is a typical example of noise or missing data combined with an affine transformation.

Table 3 is a summary of the relative errors obtained for the same four shapes of Fig. 1. Statistics for each case are computed from 20 random realizations for the noise and for 50 different starting points for missing data. The affine alignment clearly fails for the skyhawk shape, for the same reason that we did not obtain accurate results in the Euclidean case. For other shapes, we observed that the affine error is higher in comparison with the Euclidean case for the same noise and missing data. A partial explanation is that the fitting we used is not affine invariant. This is a limited source of errors since the fitting algorithm used has shown a relative robustness to affine transformation not too far from Euclidean transformations.

Compared to the Euclidean case, intrinsically, the affine coordinate system is more subject to instabilities during its computation. The conic case can be used to explain this. To compute the major and minor axis lengths of the hyperbola:  $v_1x^2 - v_2y^2 - v_3 = 0$ , we have to normalize the equation by dividing it by the term  $v_3$ , to obtain  $\frac{1}{c_1} = \frac{v_1}{v_3}$  and  $\frac{1}{c_2} = \frac{v_2}{v_3}$ . If  $v_3$  is close to zero, or small in comparison to  $v_1$  and  $v_2$ , i.e if the hyperbola is "close" to the singular case of two lines, and a small perturbation in the data set can imply that the sign of  $v_3$  (estimated by the fitting algorithm) becomes positive for a certain perturbation and negative for another one, then the sign of  $c_1$  and  $c_2$  will change, and the intrinsic coordinate system is unstable. Consequently, instability occurs around those curves which have singular covariant conics.

The car shape presents poorer results under noise than the guitar and the hiking boot. This can be explained by the fact that one of the conics factors of the fitted polynomial is close to a singular conic. This proves the need to use regularization techniques to handle such singular cases.

### 5.5. Recognition Tests

Table 4 presents the standard deviation relative to the value of every affine invariant under 0.05 standard deviation noise and 5% of missing data. As we can see, Euclidean invariants are more stable than the affine invariants. Indeed, due to the way we compute the affine invariants, by applying the inverse of the intrinsic coordinate system, the invariant robustness is directly related to the coordinate system robustness.

We can expect that the use of regularization techniques allows us to handle all the particular quartics where one step of the proposed estimations may introduce instabilities. The difficulty is that there exist many configurations that must be handled as specific cases in the decomposition and alignment computations. For example, to define a unique coordinate system, the conic factors have to be different from a circle, and the shape must not be with specific symmetries.

## 6. Conclusions

In both the Euclidean and the affine cases, using the decomposition of a quartic in three covariant

conics, we have defined a unique intrinsic coordinate system and complete sets of geometric invariants. This result is valid for most quartics.

But there are singular quartics where one step of the decomposition into covariant conics or the intrinsic coordinate system computation can not be performed uniquely. Quartics close to singular ones are generally subject to instabilities of the resulting coordinate system and invariants, under noise and missing data perturbations. This problem is not specific to our particular approach but it illustrates one difficulty of applying geometric or algebraic approaches to computer vision.

For instance, under a transformation of shape, because of noise and missing data, the model curve obtained with the fitting algorithm is not always decomposed as three conics of the same type for a shape and its transformation. In these situations, the proposed recognition approach gives bad decisions, since the model of the original and perturbed shapes are of different mathematical types.

Regularization techniques whose origins lie in the field of statistics, can be used to tackle this practical problem. Therefore, the design of the fitting algorithm must be related to the way the

intrinsic coordinate system is obtained. This implies to point all the singular quartics, and the challenge here is to design a specific fitting algorithm that biases the solution away from these singular quartics. Another important improvement will be provided by an affine invariant fitting algorithm.

The significant contribution of this paper is complete sets of geometric interpretable invariants and sets of geometric interpretable parameters for defining intrinsic coordinate systems for quartics (4th degree implicit polynomial curves) under Euclidean and affine transformations. This provides useful insights into the practical use of these polynomials in pose estimation and shape recognition. Extension to polynomials of a higher degree should contribute to a general framework for studying the application of algebraic curves and surfaces.

## References

1. G. Birkhoff and S. MacLane. *A Survey of Moderne Algebra*. The Macmillan Compagny, NYC, 1950.
2. M. M. Blane, Z. Lei, and D. B. Cooper. The 3L algorithm for fitting implicit polynomial curves and surfaces to data. *IEEE Transactions on Pattern Analysis and Machine Intelligence*, 22(3):298–313, 2000.
3. Daniel Keren, David B. Cooper, and Jayashree Subrahmonia. Describing complicated objects by implicit polynomials. *IEEE Transactions on Pattern Analysis and Machine Intelligence*, 16(1):38–53, January 1994.
4. David J. Kriegman and Jean Ponce. On recognizing and positioning curved 3-D objects from image contours. *IEEE Transactions on Pattern Analysis and Machine Intelligence*, 12(12):1127–1137, December 1990.
5. Z. Lei, D. Keren, and D. B. Cooper. Computationally fast Bayesian recognition of complex objects based on mutual algebraic invariants. In *Proceedings of IEEE International Conference on Image Processing (ICIP'95)*, volume 3, pages 635–638, 23-26 Oct. 1995, Washington, DC, USA, October 1995.
6. Z. Lei, T. Tasdizen, and D.B. Cooper. Pims and invariant parts for shape recognition. In *Proceedings of Sixth International Conference on Computer Vision (ICCV'98)*, pages 827–832, Mumbai, India, 1998. also as LEMS Tech. Report 163, Brown University.
7. J. Mundy, D. Kapur, S. Maybank, P. Gros, and L. Quan. Geometric interpretation of joint conic invariants. In J.L. Mundy and A. Zisserman, editors, *Geometric Invariance in Computer Vision*, pages 77–86. MIT Press, 1992.
8. J. Ponce, A. Hoogs, and D.J. Kriegman. On using CAD models to compute the pose of curved 3D objects. *Computer Vision, Graphics, and Image Processing*, 55(2):184–197, March 1992.
9. V. Pratt. Direct least squares fitting of algebraic surfaces. *Computer Graphics*, 21:145–152, July 1987.

10. M. Schwartz. *Information Transmission, Modulation, And Noise*. McGraw-Hill, 1990. 4th edition.
11. J. Subrahmonia, D. B. Cooper, and D. Keren. Practical reliable Bayesian recognition of 2D and 3D objects using implicit polynomials and algebraic invariants. *IEEE Transactions on Pattern Analysis and Machine Intelligence*, 18(5):505–519, May 1996.
12. S. Sullivan, L. Sandford, and J. Ponce. Using geometric distance fits for 3-D object modeling and recognition. *IEEE Transactions on Pattern Analysis and Machine Intelligence*, 16(12):1183–1196, December 1994.
13. J.-P. Tarel and D. B. Cooper. The complex representation of algebraic curves and its simple exploitation for pose estimation and invariant recognition. *IEEE Transactions on Pattern Analysis and Machine Intelligence*, 22(7):663–674, July 2000.
14. T. Tasdizen, J.-P. Tarel, and D.B. Cooper. Improving the stability of algebraic curves for applications. *IEEE Transactions on Image Processing*, 9(3):405–416, March 2000. Also as LEMS Tech. Report 176, Brown University.
15. G. Taubin. Estimation of planar curves, surfaces and nonplanar space curves defined by implicit equations, with applications to edge and range image segmentation. *IEEE Transactions on Pattern Analysis and Machine Intelligence*, 13(11):1115–1138, November 1991.
16. G. Taubin and D.B. Cooper. Object recognition based on moment (or algebraic) invariants. In J.L. Mundy and A. Zisserman, editors, *Geometric Invariance in Machine Vision*, pages 375–397. MIT Press, Cambridge, Massachusetts, 1992.
17. G. Taubin, F. Cukierman, S. Sullivan, J. Ponce, and D.J. Kriegman. Parameterized families of polynomials for bounded algebraic curve and surface fitting. *IEEE Transactions on Pattern Analysis and Machine Intelligence*, 16(3):287–303, March 1994.
18. M. Unel and W. A. Wolovich. A new representation for quartic curves and complete sets of geometric invariants. *International Journal of Pattern Recognition and Artificial Intelligence*, 13(8):1137–1149, December 1999.
19. M. Unel and W. A. Wolovich. On the construction of complete sets of geometric invariants for algebraic curves. *Advances in Applied Mathematics*, 24(1):65–187, January 2000.
20. I. Weiss. Geometric invariants and object recognition. *Int. Journal of Computer Vision*, 10(3):207–231, 1993.
21. I. Weiss. Geometric invariants and object recognition. *International Journal of Computer Vision*, 10:207–231, 1993.
22. W. A. Wolovich and M. Unel. Identifying and comparing free-form curves using implicit polynomials. LEMS Tech. Report 159, Division of Engineering, Brown University, 1997.
23. W. A. Wolovich and M. Unel. The dertermination of implicit polynomial canonical curves. *IEEE Transactions on Pattern Analysis and Machine Intelligence*, 20(10):1080–1090, 1998.





**Jean-Philippe Tarel** graduated from the École Nationale des Ponts et Chaussées, Paris, France (1991). He received his PhD degree in Applied Mathematics from Paris IX-Dauphine University in 1996 and he was with the Institut National de Recherche en Informatique et Automatique (INRIA) from 1991 to 1996. From 1997 to 1998, he was a research associate at Brown University, USA. From 1999, he is a researcher in the Laboratoire Central des Ponts et Chaussées (LCPC), Paris, France, and then from 2001 in the INRIA. His research interests include computer vision, pattern recognition and shape modeling.



**William A. Wolovich** Professor Bill Wolovich received the Ph.D. degree from Brown University in 1970, and has been on the engineering faculty there ever since. He has authored or co-authored over 90

technical papers and has written three textbooks, two in automatic control systems, and one in robotics. He has made significant contributions to the fields of multivariable control theory, robotics and image understanding. He was elected to the grade of Fellow of the IEEE in 1984 for “Contributions to the Algebraic Theory for Multivariable Control Systems, and he also is a Fulbright Fellow. Professor Wolovich received the NASA Apollo Achievement Award in 1969 for his service to the nation as a member of the team which advanced the nation’s capabilities in aeronautics and space. Professor Wolovich is a past Associate Editor of the IEEE Transactions on Automatic Control and the IEEE Journal on Robotics and Automation. He also served as a Member of the Board of Governors of the IEEE Control Systems Society. Professor Wolovich’s current research interests are in the areas of Image Understanding, Computer Graphics, Complex Dynamical Systems and Intelligent Control.



**David B. Cooper** (S '53 - M '64 - SM '90) received the BSc and ScM degrees in electrical engineering from the Massachusetts Institute of Technology,

Cambridge, Massachusetts, under the industrial co-op program in January 1957, and the PhD degree in applied mathematics from Columbia University, New York, New York, in June 1966.

From 1957 to 1966, he worked first for Sylvania Electric Products, Inc., Mountain View, California, and then for Raytheon Company, Waltham, Massachusetts, on communications and radar systems analysis at both companies. Since 1966 he has been

a professor of engineering at Brown University, Providence, Rhode Island, where he does research in pattern recognition, image understanding, stochastic 2D and 3D geometry, and applied stochastic processes.

He was joint organizer and Associate Director of the Laboratory for Engineering Man/Machine Systems (LEMS) from 1982 through 1997, and Head of Electrical Engineering for 1996 – 1998.

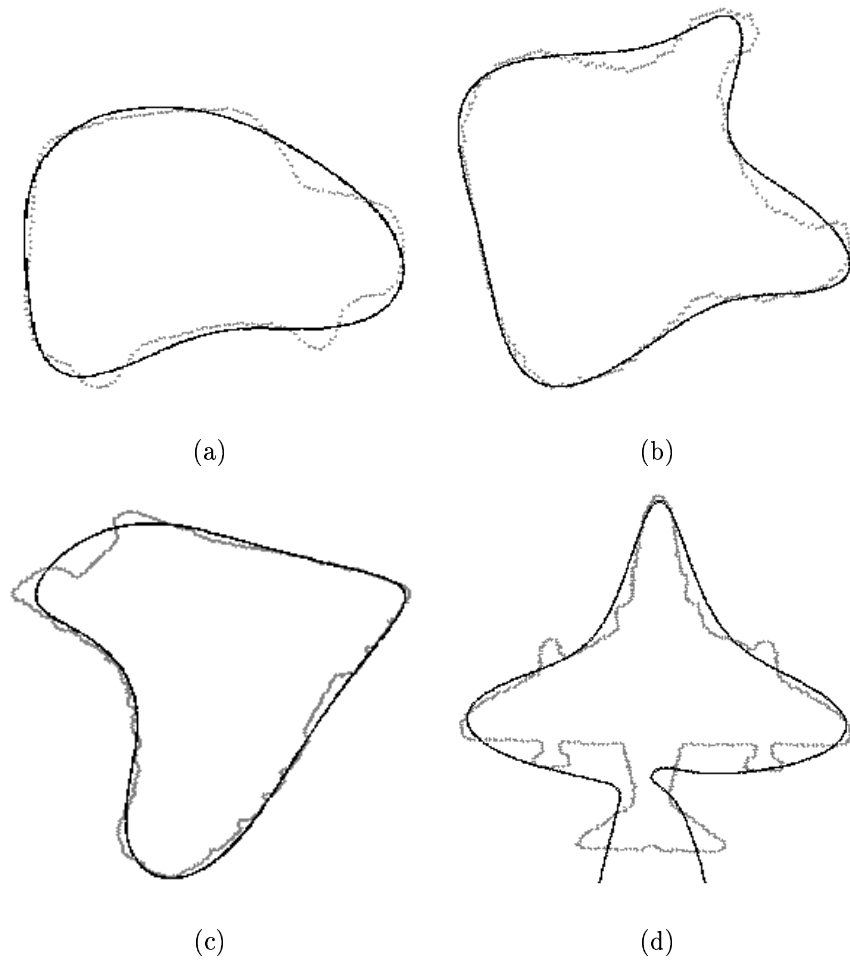
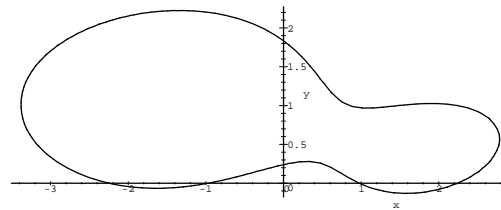
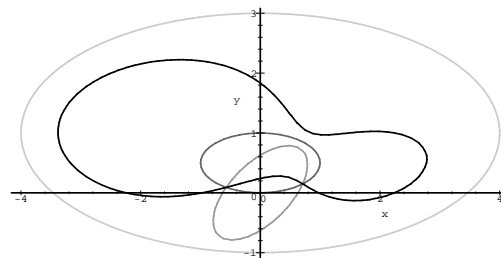


Fig. 1. Four data sets and associated quartics obtained by fitting.



(a)



(b)

Fig. 2. The quartic in (a) is decomposed into three ellipses in (b).

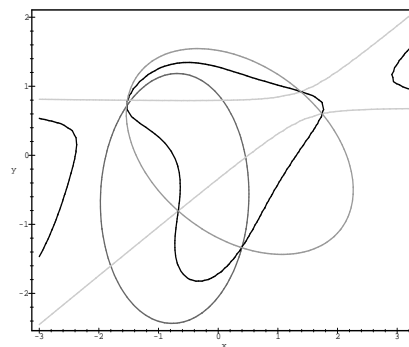
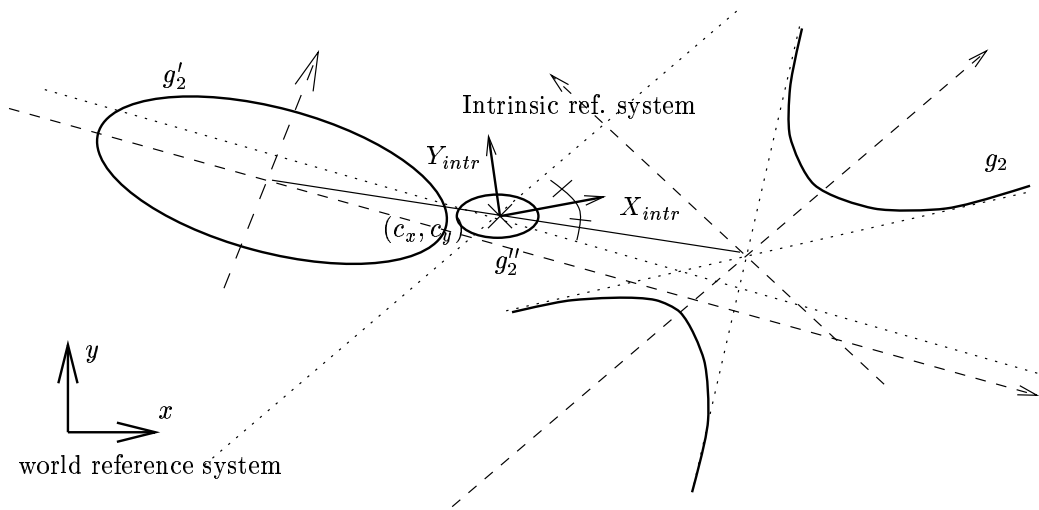
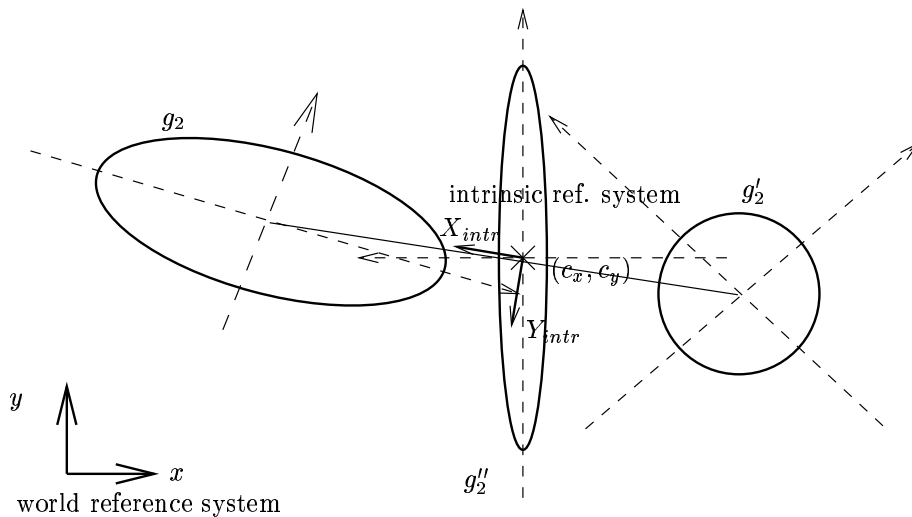


Fig. 3. The fitted quartic in Fig. 1(c) is decomposed into three covariant conics (2 ellipses and 1 hyperbola).

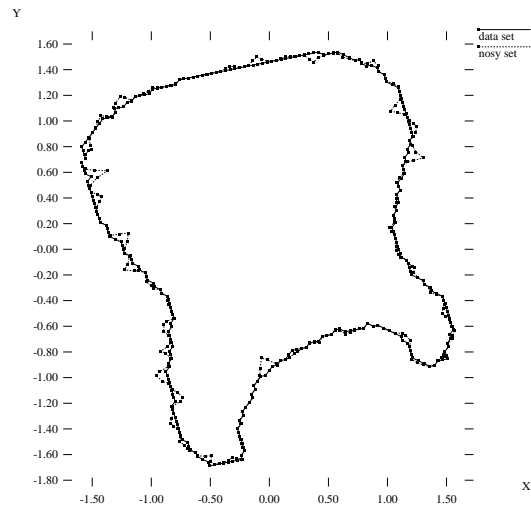


(a)

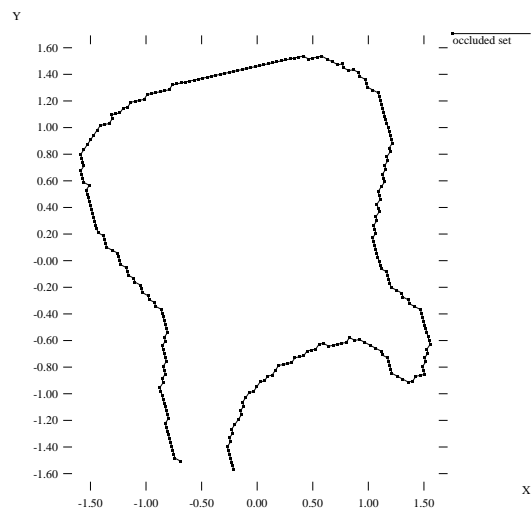


(b)

Fig. 4. Two choices of Euclidean intrinsic coordinate systems on quartics. In (a) and (b), the intrinsic center  $(c_x, c_y)$  is defined as the center of the two conic centers  $(t_x, t_y)$  and  $(t'_x, t'_y)$ . In (a), axis  $X_{intr}$  of the intrinsic coordinate system is the bisector of the two major axes of  $g_2$  and  $g_2'$ . Its orientation is assumed to be the same as that of vector  $(t_x - t'_x, t_y - t'_y)$ . Since the major axis of an ellipse is not always defined (in the case of a circle), another possible choice is shown in (b) where the  $X_{intr}$  axis is aligned with the line between points  $(t_x, t_y)$  and  $(t'_x, t'_y)$ .

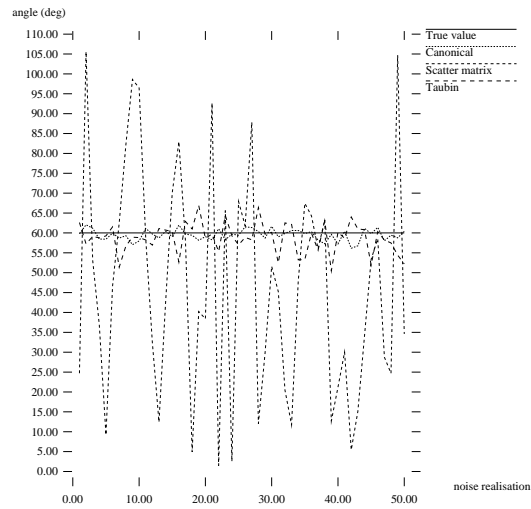


(a)

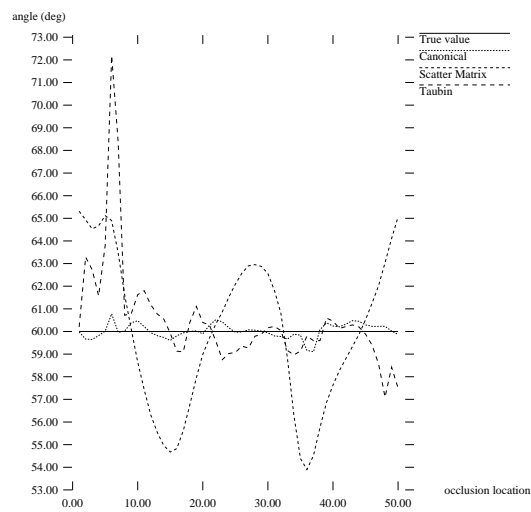


(b)

Fig. 5. In (a), the original data set of the guitar is perturbed with random Gaussian bumps at 50 different locations. The standard deviation of the noise is 0.05. The size of the shape is approximately 3. In (b), the original data has 5% missing data starting at one of the 50 possible starting points.



(a)



(b)

Fig. 6. In (a) and (b), the angle for canonical alignment are compared with our approach, Taubin’s definition, and a simple technique based on the scatter matrix of the dataset. In each case, the correct angle is 60 degrees. In (a), 0.05 std. dev. noise is added to the car and in (b), 5% of missing data is applied at each of 50 different starting points along the hiking boot.

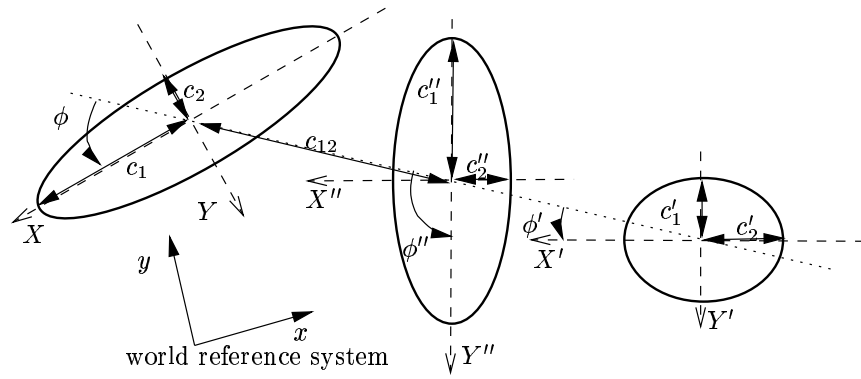


Fig. 7. An example of a complete set of Euclidean invariants for a quartic with a coordinate system defined as in Fig. 4(b).

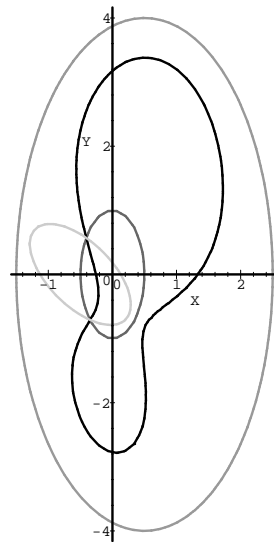


Fig. 8. The quartic of Fig. 2 in its Euclidean intrinsic coordinate system, and its three covariant conics.



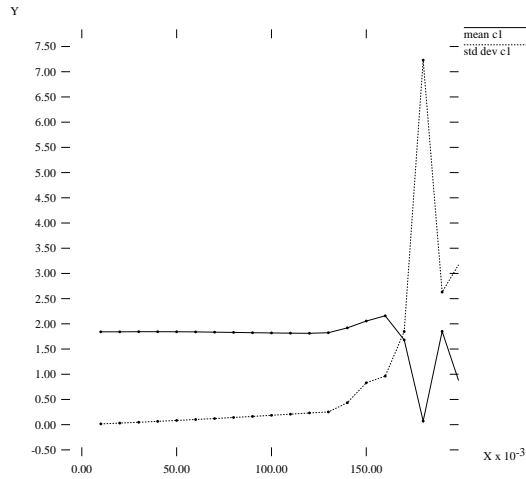
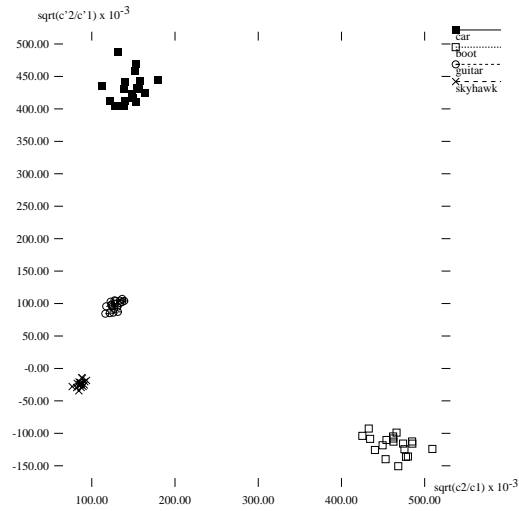


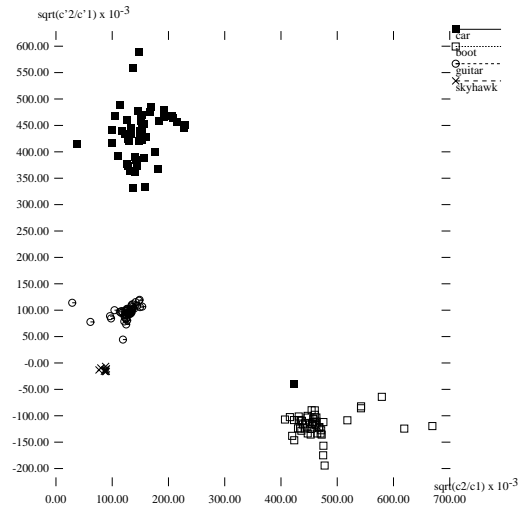
Fig. 9. Variations of the mean of  $\sqrt{|c_1|}$  and its standard deviation (with 20 realizations) for an increasing amount of perturbation with 50 bumps.

	car	guitar	boot	skyhawk	car	guitar	boot	skyhawk
$\theta$ (rad)	0.023	0.005	0.015	0.002	0.662	0.218	0.029	0.009
$c_x$	0.019	0.015	0.038	0.218	0.038	0.087	0.071	0.570
$c_y$	0.057	0.038	0.026	0.135	0.325	0.250	0.047	0.349

Table 1. The left part displays the standard deviation of the errors on the Euclidean intrinsic coordinate system under 0.05 std. dev. noise on the curve at 50 points, for 20 realizations. The right part displays the standard deviation under 5% of missing data for 50 different starting points.



(a)



(b)

Fig. 10. Distributions of invariants  $(\sqrt{|c_1/c_2|}, \sqrt{|c'_1/c'_2|})$  under 0.05 std. dev. noise (a) and 5% of missing data at 50 different starting points on the curve (b). The four data point sets used are shown in Fig. 1. Notice that the four clusters are well separated in this plane of invariants.

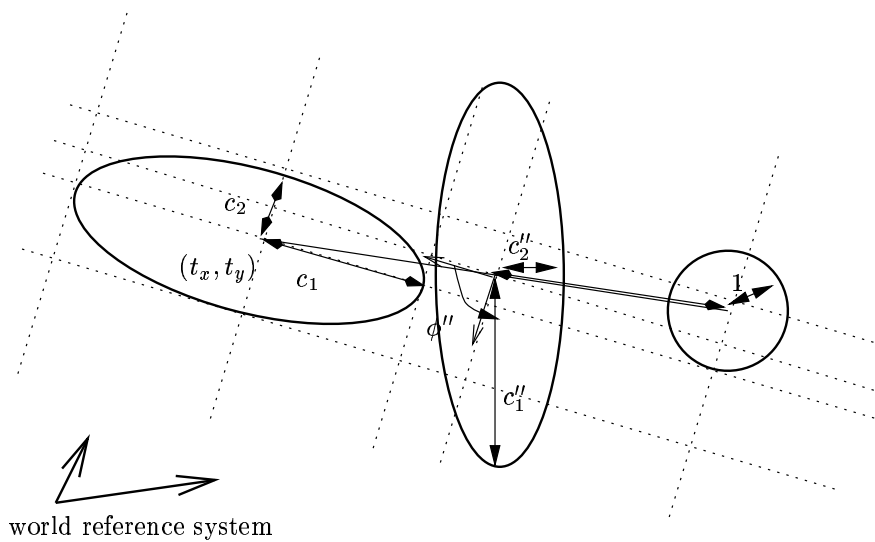


Fig. 11. This is an example of a complete set of affine invariants for quartics.

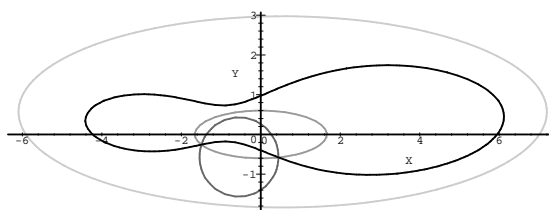
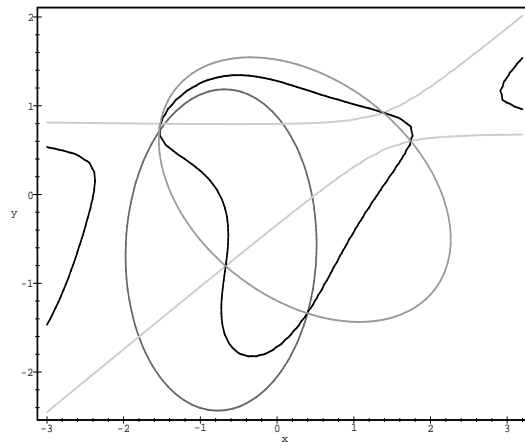
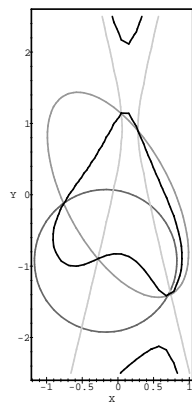


Fig. 12. The quartic of Fig. 2 in its affine intrinsic coordinate system and the three associated conics, where  $g_2^1$  is a circle.

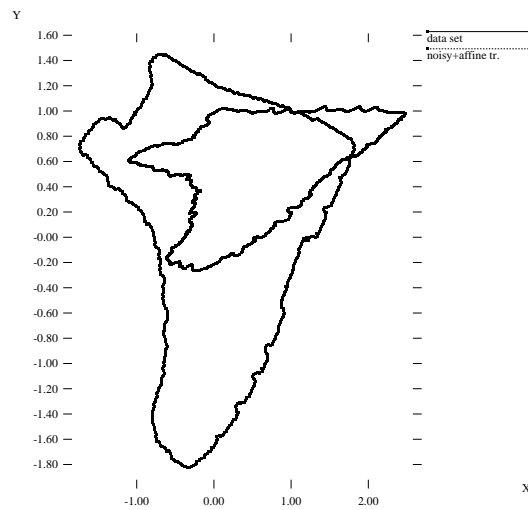


(a)

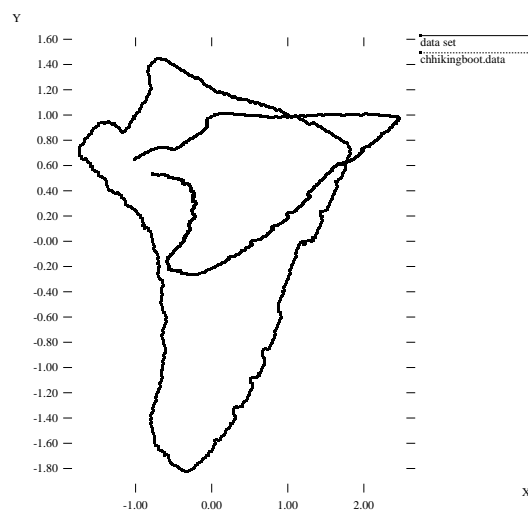


(b)

Fig. 13. Decomposition into three conics of the quartic fitted on the hiking boot in the original coordinate system (a) and its affine intrinsic coordinate system (b).



(a)



(b)

Fig. 14. In (a) are shown the original data set of the hiking boot and its perturbation with random Gaussian bumps of size 0.05 (shape of size 3). In (b) are shown the original data and its perturbation with 5% of missing data. In each case, an affine transformation is applied on the perturbed shape.

	car	guitar	boot	skyhawk	car	guitar	boot	skyhawk
$c_1$	11.9%	1.7%	4.6%	151%	33.7%	40.9%	6.3%	911.2%
$\frac{c_2}{c_1}$	10.8%	4.8%	4.4%	4.3%	33.4%	16.1%	10.3%	10.2%
$\frac{c'_1}{c_1}$	12.7%	5.5%	130%	45.9%	283%	19.8%	286%	2232%
$\frac{c'_2}{c'_1}$	5.1%	7.3%	12.3%	20.3%	19.4%	12.9%	18.3%	62.8%
$\frac{c''_1}{c_1}$	17.3%	5.4%	9.8%	62.2%	741%	507%	20.4%	14948%
$\frac{c''_2}{c''_1}$	13.7%	6.9%	10.3%	26.8%	50.8%	18.0%	14.8%	250%
$\phi$	2.5%	0.8%	2.8%	0.8%	5.4%	1.3%	3.7%	1.5%
$\phi'$	2.5%	0.8%	2.8%	0.8%	5.4%	1.3%	3.7%	1.5%
$\phi''$	3.9%	19.4%	7.1%	0.9%	26.9%	65.4%	10.8%	3.5%
$c_{12}$	6.0%	8.4%	2.5%	15.6%	21.1%	64.4%	4.0%	33.0%
$c$	15.8%	9.7%	497%	72.4%	691%	101%	553%	623.2%

Table 2. Percentage of relative errors on invariants estimations under 0.05 std. dev. noise (left) and 5% missing data on the curve at 50 different starting points (right).

	car	guitar	boot	skyhawk	car	guitar	boot	skyhawk
$a$	30.6%	6.2%	5.2%	683.8%	5860%	12.2%	7.2%	290%
$b$	35.5%	7.2%	6.4%	479.8%	205%	13.1%	9.3%	409%
$c$	45.5%	4.2%	5.1%	108.5%	187%	5.8%	6.1%	57.4%
$d$	44.4%	5.7%	80.9%	79.5%	204%	8.7%	70.0%	59.4%
$c_x$	17.9%	4.8%	3.4%	18.9%	36.0%	7.1%	6.1%	16.7%
$c_y$	0.9%	2.5%	1.8%	24.1%	3.6%	5.8%	3.1%	21.7%

Table 3. Percentage of errors in the estimated affine coordinate system under 0.05 of noise (left) and 5% of missing data (right).

	car	guitar	boot	skyhawk	car	guitar	boot	skyhawk
$c_1$	299%	12.8%	10.8%	424%	852%	21.3%	17.3%	699%
$\frac{c_2}{c_1}$	49.1%	7.7%	13.6%	126%	65.6%	12.3%	49.7%	75.3%
$t_x$	63.6%	25.5%	16.2%	69.0%	232%	50.2%	32.3%	698%
$t_y$	37.3%	11.8%	5.1%	302%	241%	26.5%	6.0%	53.3%
$\frac{c_1''}{c_1}$	17.7%	11.1%	66.7%	274%	87.3%	16.2%	211%	432%
$\frac{c_2''}{c_1''}$	81.3%	4.4%	15.5%	117%	43.1%	5.3%	17.7%	2211%
$\phi''$	23.5%	36.4%	4.2%	651%	149%	39.4%	14.2%	1650%
$c$	10.4%	13.8%	43.3%	106%	597%	28.1%	120%	3057%

Table 4. Percentage of errors in invariants estimation under 0.05 std. dev. noise (left) and under 5% missing data (right).